Small-scale cyclically thermally-activated pile under inclined mechanical loads

Aylin Nouri, Ali Noorzad, Jean-Michel Pereira, Anh Minh Tang

Small-scale cyclically thermally-activated pile under inclined mechanical loads

Author 1

- Aylin Nouri, Ph.D. candidate, MSc
- Faculty of Civil, Water and Environmental Engineering, Shahid Beheshti University (SBU), Tehran, Iran
- Navier, Ecole des Ponts, Univ Gustave Eiffel, CNRS, Marne-la-Vallée, France
- i_noori@sbu.ac.ir; aylin.nouri@enpc.fr
- https://orcid.org/0000-0001-8854-0578

Author 2

- Ali Noorzad, Associate Professor, Ph.D., P. Eng.
- Faculty of Civil, Water and Environmental Engineering, Shahid Beheshti University (SBU), Tehran, Iran
- a_noorzad@sbu.ac.ir
- https://orcid.org/0000-0002-3785-7679

Author 3

- Jean-Michel Pereira, Professor, Ph.D.
- Navier, Ecole des Ponts, Univ Gustave Eiffel, CNRS, Marne-la-Vallée, France
- jean-michel.pereira@enpc.fr
- https://orcid.org/0000-0002-0290-5191

Author 4

- Anh Minh Tang, Research Director, Ph.D.
- Navier, Ecole des Ponts, Univ Gustave Eiffel, CNRS, Marne-la-Vallée, France
- anh-minh.tang@enpc.fr
- https://orcid.org/0000-0002-7149-8497

Full contact details of corresponding author.

Dr. Ali Noorzad

Faculty of Civil, Water and Environmental Engineering, Shahid Beheshti University (SBU)

Hakimieh, East Vafadar Boulevard, Tehran, Iran

Email : a_noorzad@sbu.ac.ir

Phone: +98-21-7731-3062

Fax : +98-21-7700-6660

Acknowledgements

The first and second authors would like to express their gratitude to the Niroo Research Institute (NRI) for funding the present study, which is a part of the research project entitled, “Safety assessment of energy piles” (Project No. 99/51304/178). The first author is also funded as a visiting scholar by the Iranian Ministry of Science, Research and Technology, and the French Foreign Ministry. The financial support from these funding sources is greatly appreciated.

Small-scale cyclically thermally-activated pile under inclined mechanical loads

Abstract: In this study, a series of 1-g physical model tests was carried out using an instrumented model energy pile installed in dry sand to characterize the influence of cyclic thermal loading on the response of energy pile subjected to inclined mechanical loading. The loading scheme considered in the model tests comprised a pre-applied axial load (10, 20, and 40% of the ultimate axial load) combined with a horizontal load (30, 50, and 70% of the ultimate horizontal load) followed by ten thermal cycles with temperature variation of ± 1 °C. The results indicated that imposing thermal cycles to the pile subjected in advance to inclined mechanical loading resulted in a pile head irreversible settlement and horizontal displacement, which would gradually accumulate over thermal cycles. By the end of the tenth thermal cycle, the amount of accumulated irreversible settlement and horizontal displacement were generally in the range of 0.1-0.6% and 1.1-2.3% of pile diameter, respectively. Under the same horizontal load, thermal cycles at a higher axial load induced a higher irreversible settlement but a lower horizontal displacement at the pile head. Under the same axial load, thermal cycles at a higher horizontal load induced a lower settlement but a higher horizontal displacement at the pile head. Despite the fact that ultimate horizontal bearing capacity of pile remained unchanged after ten thermal cycles, it is recommended that due to the accumulation of irreversible horizontal displacement during the cyclic thermal loading, the long-term performance of energy pile is controlled by horizontal displacement rather than capacity.

Keywords: Thermo-mechanical behavior, Energy pile, Physical model, Inclined mechanical load, Cyclic thermal load.

List of notations

ρ_s	Particle density
e_{max}	Maximal void ratio
e_{min}	Minimal void ratio
D_{50}	Mean grain size
F_v	Pile head axial load
F_h	Pile head horizontal load
Q_v	Ultimate axial load of the pile
Q_h	Ultimate horizontal load of the pile

D	Outer diameter of model pile
L	Length of pile
ε_T	Thermal strain
n	length scaling factor (prototype divided by model)
α_p	Thermal expansion coefficient of the prototype-scale pile
α_m	Thermal expansion coefficient of the model-scale pile
ΔT_p	Temperature change in the prototype-scale pile
ΔT_m	Temperature change in the model-scale pile
a	Soil thermal diffusivity
G	Soil stiffness
E	Elastic modulus
I	Moment of inertia

1. Introduction

In the last few decades, to preserve the future generations from energy crises, significant effort has been accomplished to collect energy from renewable sources, including shallow geothermal energy. Geothermal energy piles are one of the most common and efficient systems of shallow geothermal energy, in which geothermal loops are integrated into the foundation elements to extract/inject the heat from/into the ground with the purpose of meeting the building heating and/or cooling demands. Since the mid-1980s, when the first energy piles were installed in Austria, the use of energy piles has increased rapidly in many countries, including Canada, Australia, Europe, UK, and China [1-7]. Even though lots of successful energy pile projects have been implemented in a variety of important structures such as high rise buildings, underground transport projects and earth retaining structures in the world, the application of this technology is still limited in the energy industry and the true potential for adoption of energy piles is yet to be realized in highway bridges for deck de-icing and offshore platforms for combined exploitation of offshore wind, wave and geothermal energy. In such applications, energy piles could be subjected not only to axial loads, but also to cyclic horizontal loads and moments due to heavy wind, earthquakes, earth pressure, slope failure, lateral spread induced by liquefaction and wave and current forces on offshore structures.

In the current design practice, the response of conventional pile under combined axial and horizontal loading is separately analyzed and then superposed. This approach neglects the coupling effect while the optimum design of pile foundations requires consideration of the influence of axial loads on their horizontal response. Most of previous studies have investigated the behavior of conventional piles under pure horizontal loads. Only a limited number of studies have investigated the response of conventional piles subjected to inclined loading using physical modelling under single gravity [8-13] or multiple gravities [14] and field-scale tests [15-17]. Early studies, using physical model, presented by Jain *et al* [8] and Lee *et al* [9,10] suggested an increase in pile head horizontal displacement in the presence of axial loading. That was in contrast to the findings of more recent studies presented by Mu *et al* [11], Lu & Zhang [14], Xu *et al* [12] and Zhang *et al* [13]. There is still a lot of complexities and uncertainties pertinent to the coupling effects even on the conventional pile behavior. That might be intensified in the case of energy piles because the thermal variations could affect the energy pile-soil interaction behavior, e.g., causing ratcheting

phenomena in case of cyclic thermal loads. Therefore, it is necessary to identify the influence mechanism of axial compression loads on the horizontal behavior of energy piles.

As for traditional piles, the studies conducted so far have concentrated on the separate investigation of axial and horizontal responses of energy piles neglecting the coupling effects on the thermally-induced displacements in both axial and horizontal directions. Many researchers have put a lot of effort to better understand the thermo-mechanical behavior of energy piles during monotonic heating or cooling and one or multiple thermal cycles. The works of Vitali *et al* [18] and Zhao *et al* [19] could be considered as the only available studies investigating the influence of monotonic heating and heating-cooling cycles on the flexural behavior of horizontally-loaded energy piles, respectively. Several studies have been performed to assess the behavior of axially-loaded energy piles during multiple thermal cycles through field scale tests [20-25], 1-g small-scale physical model tests [26-36] and centrifuge model tests [37-41]. Dry sand was the most common type of soil used in these small-scale physical model tests. The above-mentioned studies indicated that imposing thermal cycles upon the axially-loaded semi-floating energy piles results in cumulative irreversible settlement, which has been identified qualitatively similar in 1-g small-scale physical model tests and in centrifuge testing, even though quantitative differences have been observed. Therefore, despite the inherent limitations of 1-g small-scale physical model tests compared to the field-scale and centrifuge model tests, qualitative results obtained from the former could be used to gain an insight into the behavior of energy piles under thermo-mechanical loading and the mechanism involved. Overall, model tests to analyze the performance of energy piles subjected to combined mechanical and cyclic thermal loads are still limited and there is a necessity to deeply investigate the potential effects of multiple thermal cycles on the energy pile-soil interaction mechanism.

The objectives of the present research are twofold: (1) investigating the influence of multiple heating-cooling cycles on the geotechnical responses of energy piles; (2) evaluating the coupling effects on the thermally-induced mechanical response of energy piles. Therefore, a series of 1-g model experiments was carried out on a single model energy pile embedded in dry sand. The model pile was initially subjected to axial static compressive load (10, 20, and 40% of the ultimate axial load); in the subsequent stage, horizontal static load was incrementally applied (30, 50, and 70% of the ultimate horizontal load), while the axial load was kept constant. At each level of horizontal load, to simulate the actual operating condition of energy piles, repeated ten thermal cycles with temperature

variation in the range of ± 1 °C were applied to the pile while the mechanical loads were maintained constant. The obtained results, including pile temperature, soil temperature, horizontal and axial displacements of pile head were finally analyzed and discussed.

2. Experimental approach

2.1 Experimental setup

The schematic view of the experimental setup is depicted in Fig. 1. To obtain a correct physical modeling, the material type and dimensions of the model pile are selected by maintaining the dimensionless ratio of $\phi_1 = \frac{GL^4}{EI}$ identical in the model and the prototype piles (G= soil stiffness; E =elastic modulus; I = moment of inertia; L=length of pile). Since the soil stiffness scales as $\left(\frac{1}{n}\right)^{\lambda}$ in 1-g model testing (λ = 0.5 for sandy soils; n = length scaling factor), the bending stiffness, EI, would scale as $\left(\frac{1}{n}\right)^{4.5}$ [42]. In the present study, a closed-end aluminum tube having an outer diameter (D) of 20 mm, inner diameter of 18 mm, embedded length of 600 mm, and thermal expansion coefficient of 22.2×10^{-6} /℃ was selected as the model pile with a length scaling factor of 20. This is used to simulate the prototype pile of 570 mm diameter solid section made of reinforced concrete with a compressive strength of 30 MPa. Since the scaling of pile diameter depends on the scaling of pile bending stiffness, the diameter and length of the pile could not be scaled in the same way. According to Das [43], for the properties of sand and pile selected in this study, model pile having the length to diameter ratio (L/D) of 30 behaves as a long flexible pile during horizontal loading at 50% relative density of the sand. Therefore, in response to horizontal loading, the model pile is expected to bend from the top. A cylindrical steel tank with a diameter of 548 mm ($\approx$ 27D) and a height of 980 mm was used as a soil tank, in which the distance between the pile toe and the base of the model container was equal to 340 mm ($\approx$ 17D). It is inferred from the literature that with a tank-to-pile diameter ratio of 10D and a soil cushion with a depth of 3-4D below the pile toe, boundary effects of the tank could be considered negligible while testing the model pile under a combination of axial, horizontal and thermal loads [29,44-49]. In order to mimic the roughness of the prototype pile surface, the surface of the model pile was coated with sand. It is to be noted that the attached sand layer would not change the axial and flexural stiffness of the pile.

106 Expanded polystyrene sheets were wrapped around the soil tank to insulate it against heat exchange between the soil
107 and the ambient air.
108
109 The soil used for this study was dry Fontainebleau NE34 sand with the following physical properties [50]: mean
110 grain size $D_{50} = 0.21$ mm, particle density $\rho_s = 2.65$ Mg/m^3, maximal void ratio $e_{max} = 0.884$; minimal void
111 ratio $e_{min} = 0.557$. In the developed model, the ratio between the pile diameter (20 mm) and the mean grain size
112 (0.21 mm) was equal to 95. The mentioned ratio was greater than the suggested limit by Fioravante [51], thereby the
113 grain-size scaling effect could be considered negligible. A wooden tamper was used to compact the dry sand to a
114 density of 1.54 Mg/m^3 (that corresponds to a relative density of 50%). Before installation of the model pile, the sand
115 was placed and compacted in seven 50-mm-thick layers in the tank. After the compaction of these layers, a steel bar
116 was mounted and bolted to the upper surface of the soil tank as a temporary support for installing the model pile at
117 the center of the tank. Compaction of the remaining soil around the fixed pile was then continued by 50-mm-thick
118 layers except for the top layer, which had a thickness of 40 mm. The density was controlled by the mass of soil
119 being compacted and the thickness of each layer. The above-mentioned experimental setup and method of sand
120 samples preparation have already been adopted by Kalantidou *et al* [26], Yavari *et al* [27] and Nguyen *et al* [29].
121 The repeatability of these studies confirms the uniformity of sand samples prepared by this method.

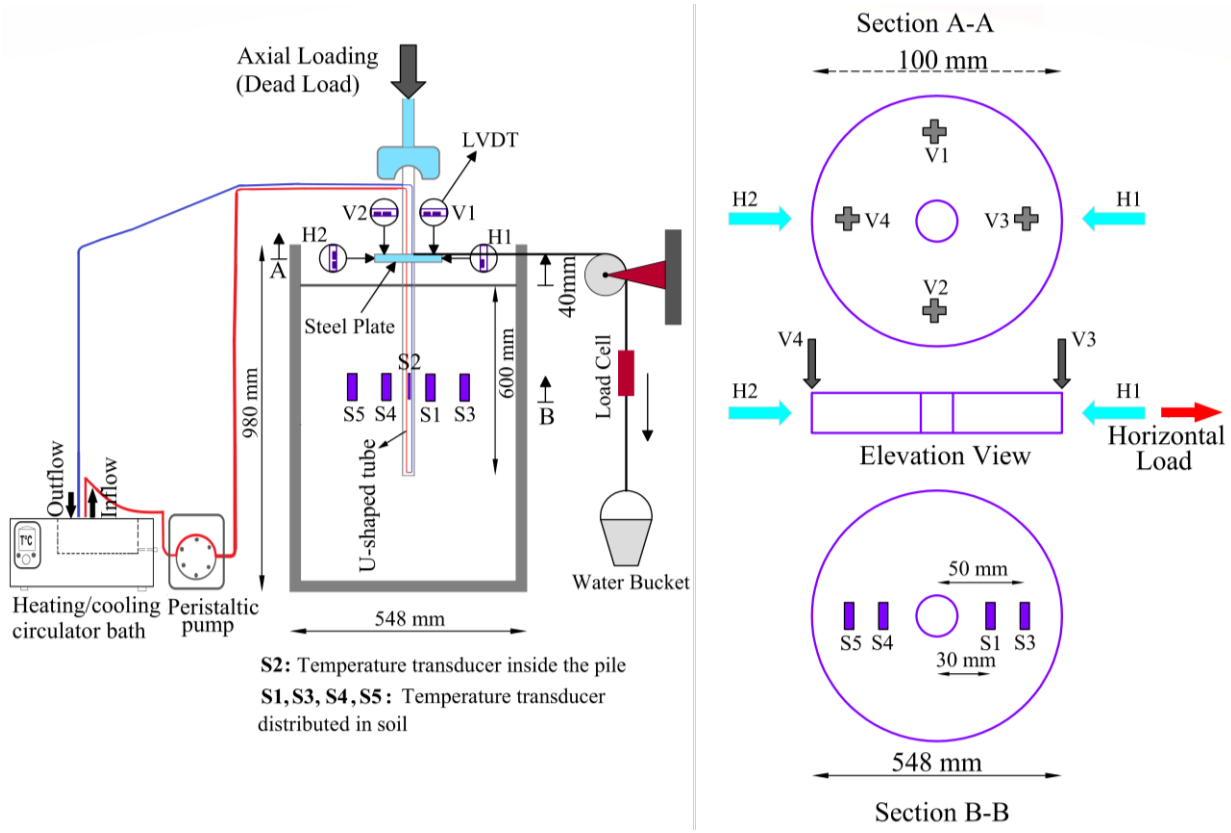

Fig. 1. Schematic view of experimental setup.

To control the pile temperature, model pile was equipped with an aluminum U-shaped tube (2 mm inner diameter and 3 mm outer diameter) linked to a temperature-controlled water bath and a peristaltic pump. The annulus between the pile and the aluminum U tube was filled with water to improve the heat transfer. Yavari *et al* [27] indicated that the temperature changes measured at different depths of soil and at the same distance from the pile are quite similar. Hence, it could be concluded that the temperature of the shallow soil layers is not influenced by the ambient temperature, even though the soil surface is not insulated against heat exchange. Therefore, in the present study, pile and soil temperatures were only measured by the temperature sensors (*S1*-*S5*) placed at a depth 300 mm below the soil surface and at distances of 30 mm (≈ 1.5D) and 50 mm (≈ 2.5D), respectively, from the pile axis (as shown in Fig. 1).

The loading system, which had been previously adopted by Kalantidou *et al* [26], Yavari *et al* [27], and Nguyen *et al* [29], was modified to consider the horizontal load. The static axial compressive load was applied to the model pile by placing dead weights on the pile head and the static horizontal load was applied to the pile in increments by

allowing water flow in the plastic bucket linked to the pile head through a piece of rope over a pulley. The flow rate was controlled by a valve attached to the water tank. The applied horizontal load and pile head displacements were measured accurately using a load cell and displacement transducers (*V1-V4, H1-H2*), respectively.

2.2 Test program

In the present work, nine experiments were performed (Table 1), each one corresponds to a soil sample. In the test ID, notations of E and T denote the experiment (E) performed on one soil mass, and subtests (T) of the main experiment, respectively. Notations of M and TM after the first number denote loading type in experiments, i.e. mechanical loading (M), and thermo-mechanical loading (TM), respectively. The number after notations of E or T is the amount of pre-applied axial load (percent compared to ultimate axial load), and the number after notations of M or TM is the amount of applied horizontal load (percent compared to ultimate horizontal load).

Actually, for experiment E40M (and test T40M), after the installation of the setup, axial load (F_v) was first applied to 40% of the ultimate axial load (Q_v, which was estimated at 500 N by Nguyen *et al* [29] using the same system and the same soil). Afterward, the horizontal load (F_h) was increased progressively until failure (assumed to occur when pile head horizontal displacement exceeds 20%D). This value is in the range of pile horizontal displacements (at the sand bed surface level) often used to estimate the ultimate horizontal load capacity value [49,52]. The aim of experiment E40M (and test T40M) was to determine the mechanical behavior (and the ultimate horizontal load Q_h) of the pile under the increase of horizontal load while the axial load was maintained at 40% Q_v. Experiment E40M_R (and test T40M_R) is the replicate of experiment E40M (and test T40M). Experiments E20M (and test T20M) and E10M (and test T10M) are similar to E40M (and test T40M) but with F_v equal to 20% and 10% Q_v, respectively. Experiments E20M_R and E10M_R are their replicates.

Table 1. Test program.

Experiment	Test	F_v / Q_v (%)	F_h / Q_h (%)	Number of thermal cycle
E40M	**T40M**	**40**	**>100**	**0**
E40M_R	**T40M_R**	**40**	**>100**	**0**

E40TM	**T40TM_30**	**40**	**30**	**10**
	T40TM_50	**40**	**50**	**10**
	T40TM_70	**40**	**70**	**10**
E20M	**T20M**	**20**	**>100**	**0**
E20M_R	**T20M_R**	**20**	**>100**	**0**
E20TM	**T20TM_30**	**20**	**30**	**10**
	T20TM_50	**20**	**50**	**10**
	T20TM_70	**20**	**70**	**10**
E10M	**T10M**	**10**	**>100**	**0**
E10M_R	**T10M_R**	**10**	**>100**	**0**
E10TM	**T10TM_30**	**10**	**30**	**10**
	T10TM_50	**10**	**50**	**10**
	T10TM_70	**10**	**70**	**10**

In order to simulate typical load combinations of energy piles implemented in high-rise buildings, highway bridges, earth-retaining structures and those located on sloping ground, the loading scheme of model tests in the present study comprised pre-axial static loading followed by horizontal static loading before subsequent heating-cooling cycles. In such a loading scheme, the additional rotational restraint induced by pile cap, group effects and the cyclic nature of horizontal loading were not taken into consideration to isolate the coupling effects on the energy pile behavior during cyclic thermal loading. Therefore, for experiment E40TM, F_v was first increased to 40% Q_v, followed by an increase of F_h to 30% Q_h. Afterward, under this inclined mechanical load, thermal cycles were applied (test T40TM_30). Owing to the fact that the pile temperature was controlled manually in the experiments, a duration of 2 h was adopted for the heating and cooling phases, which was long enough for the soil temperature to reach equilibrium according to the temperature history of soil obtained by Nguyen *et al* [29] using identical pile and soil under the same temperature change applied to the pile. Therefore, in each thermal cycle, pile temperature was manually increased from an ambient temperature of 22 ℃to 23 °C over a 2-h heating phase prior to being decreased to 21 °C over a 2-h cooling phase. Finally, during the recovery phase, it was rapidly increased to an ambient

temperature of 22 ℃ and maintained over 20 h prior to the subsequent thermal cycle. For the tests continued during the weekends, the duration of the recovery phase of some thermal cycles was increased to more than 20 h.

To scale the heat diffusion time in thermal cycles, Fourier's number could be used [48]:

$$\left(\frac{at}{(D/2)^2}\right)_m = \left(\frac{at}{(D/2)^2}\right)_p \quad (1)$$

Where a, t, and D are soil thermal diffusivity, heat diffusion time, and pile diameter, respectively. The subscripts "m" and "p" mean model and prototype, respectively. Since the same sand was considered in model and prototype scale, the scaling factor for soil thermal diffusivity is one. Hence, the heat diffusion time must be scaled by $\left(\frac{D_p}{D_m}\right)^2$.

As already noted by Zhao *et al* [54], thermal strains ($\varepsilon_T = \alpha \Delta T$) should be scaled by the same scaling factor as mechanical strains (i.e. $N^{0.5}$). Hence, the temperature changes in the prototype-scale concrete pile (ΔT_p) are given by:

$$\Delta T_p = N^{0.5} \times \frac{\alpha_m \Delta T_m}{\alpha_p} \quad (2)$$

Since the model-scale aluminum pile has a thermal expansion coefficient (α_m) of 22.2×10^{-6} /℃, which is 2.2 times that (α_p) of a prototype-scale concrete pile, temperature changes of $\pm$1℃ (ΔT_m) during 2-h heating and cooling phases in the model-scale pile could simulate temperature changes of $\pm$10℃ during 2.25-month heating and cooling phases in the prototype-scale pile. This temperature variation range of the prototype pile is within the range of 3-37 °C of field-scale energy piles [25,53].

four hours of temperature changes of $\pm$1℃ in the model-scale pile (ΔT_m) could simulate five months of temperature changes of $\pm$10℃ in the prototype-scale pile.

After performing test T40TM_30, F_h was increased to 50% and 70% Q_h prior to the application of the thermal cycles in tests T40TM_50 and T40TM_70, respectively. Experiments E20TM and E10TM are similar to E40TM but with F_v equal to 20% and 10% Q_v, respectively. Normally, in each thermo-mechanical test (TM), model pile was

subjected to 10 heating-cooling cycles over a period of two weeks. There were two reasons to simulate the cyclic thermal load using 10 heating-cooling cycles. First, each heating-cooling cycle required about one day for completion and hence, in order to investigate different loading conditions, the number of thermal cycles should be optimized. Second, the results obtained from the first thermo-mechanical test (test T10TM_30) indicated that the increment rate of irreversible displacement in both axial and horizontal directions is unsteady during the first thermal cycles and, as the number of thermal cycles increased, it tended to be stable. To measure pile head axial displacement, in all experiments except E20M_R and E40M_R, axial displacement sensors *V1* and *V2* were mounted in the perpendicular direction to horizontal load and opposite to each other at a distance of 40 mm from the pile axis. Conversely, in experiments E20M_R and E40M_R, axial displacement sensors *V3* and *V4* were mounted in the horizontal load direction and opposite to each other at a distance of 40 mm from the pile axis. In all experiments, pile head horizontal displacement was measured at a height of 40 mm above the soil surface by two horizontal displacement sensors (*H1* and *H2*) mounted directly opposite to each other at a distance of 50 mm from the pile axis (see Fig. 1).

3. Results and discussions

3.1. Load-displacement response of the model pile subjected to purely mechanical load

In the mechanical experiments, the data collected in terms of axial load and settlement of the model pile while being subjected to pure axial loading are plotted in Fig.2. The load-settlement curves corresponding to the previous studies conducted using identical pile and soil are drawn in the same figure for comparison purpose [27,29]. It is clearly seen that the measured settlements in the present study is similar to those reported in previous works, confirming the repeatability of the model preparation and loading system.

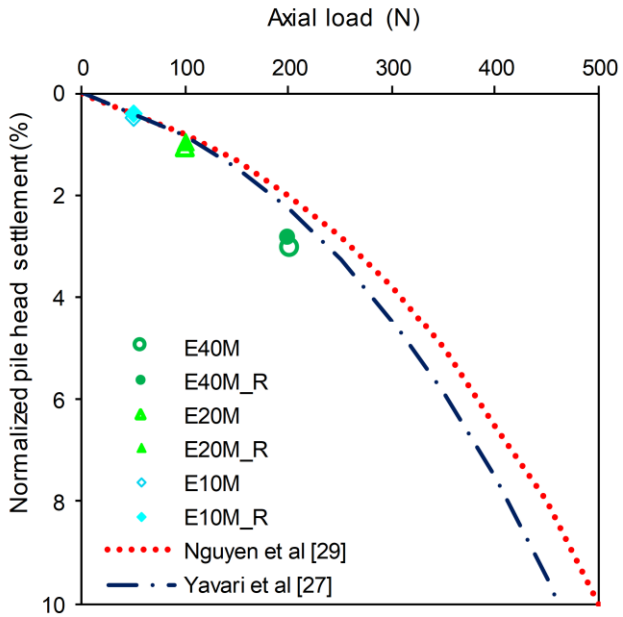

Fig. 2. Pile head settlement versus axial load measured in mechanical tests without horizontal loading.

Fig. 3(a) presents the normalized pile head horizontal displacement (i.e. divided by the pile diameter) versus the horizontal load while the axial load is maintained constant for all tests. The similarity of the horizontal load-horizontal displacement curves obtained from replicate tests indicates the high repeatability of the experimental procedure. All the results show an increase of pile head horizontal displacement while the horizontal load is increased. The ultimate horizontal load (corresponding to a normalized pile head horizontal displacement of 20%D) is equal to 86 - 90 N. An increasing pre-applied axial load from 10% to 20% Q_v causes a negligible reduction in pile head horizontal displacement, which agrees with the findings of previous studies using similar soil conditions and experimental set-up [11-14]. On the contrary, with an increase of pre-applied axial load to 40% Q_v, pile head horizontal displacement increases rather than decreases further so that the horizontal load-horizontal displacement curve is almost the same as the case of the pre-applied axial load of 10% Q_v. Overall, where axial load varies between 10% and 40% Q_v, the horizontal behavior of the pile is almost independent of the axial load. It is likely that small pre-applied axial loads ($F_v \leq 40\%Q_v$) have negligible influence on the horizontal soil resistance.

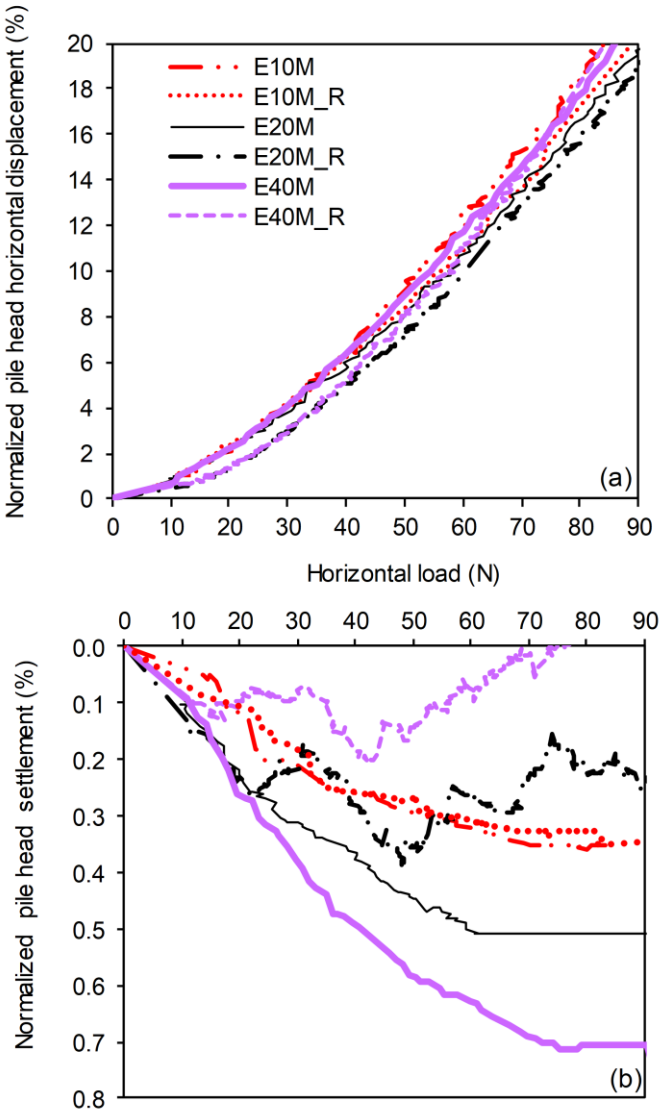

Fig. 3. Variation of (a) pile head horizontal displacement; (b) pile head settlement with horizontal load measured under constant axial load.

Fig. 3(b) indicates the relationship between the horizontal load and normalized pile head settlement of the same tests. It can be observed that the settlement of experiments E20M and E40M are significantly different to those of their replicates. As mentioned earlier, in experiments E20M and E40M, pile head settlement was measured by displacement sensors V1 and V2, while in their replicates (i.e. E20M_R and E40M_R), it was measured by displacement sensors V3 and V4. Therefore, it is worthy to note that as the model pile starts bending from the top in response to the horizontal load, the settlement measured by displacements sensors V3 and V4 does not accurately represent the settlement at the pile head. If the experiments using displacement sensors V3 and V4 (i.e. E20M_R and

E40M_R) are ignored, it could be observed that normalized pile head settlement increases at a reducing rate with increasing horizontal load, and tends to stabilize at 0.35%, 0.50%, and 0.70% at high horizontal load under constant axial load of 10% Q_v (E10M, E10M_R), 20% Q_v (E20M), and 40% Q_v (E40M), respectively. This behavior is similar to that obtained in the experimental study of Lu & Zhang [14]. This can be explained by the fact that when the pile has not moved sufficiently in the horizontal direction, the mobilization of passive earth pressure in front of the pile does not compensate for the loss of active earth pressure behind the pile. Thereby, the resulting shaft resistance loss and interface slip lead to the transfer of axial compressive load from the shaft to the pile toe and causes the increase in the pile toe settlement and resistance.

3.2. Influence of cyclic thermal loading on the behavior of the model pile subjected in advance to inclined mechanical loading

Fig. 4 illustrates the histories of measured temperature of model pile and surrounding soil at various distances from the pile axis for the first thermal cycle of Test T40TM_30. As shown in Fig. 4, when the pile temperature rises up from 22 ℃ to 23 ℃ during the heating phase and decreases to 21 ℃ during the subsequent cooling phase, the variation of soil temperature recorded at 30 mm (*S1* and *S4*) and 50 mm (*S3* and *S5*) from the pile axis have a smaller amplitude, ±0.5 ℃ and ±0.2 ℃, respectively. The same phenomenon was also observed by Ng *et al* [40] and Nguyen *et al* [29]. It is important to note that for all thermal cycles in the thermo-mechanical tests, the measured temperatures in the model pile and surrounding soil follow the same trend as observed for the first thermal cycle of Test T40TM_30. Additionally, during the recovery phase, the temperatures of the model pile and the surrounding soil return gradually to the ambient temperature.

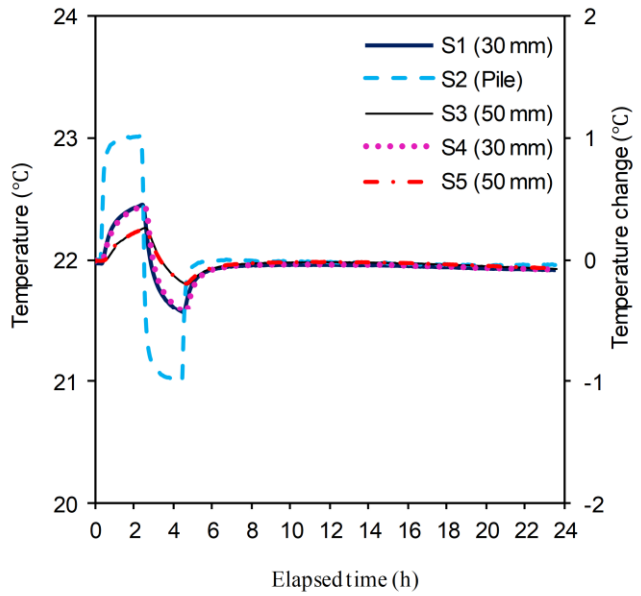

Fig. 4. Soil and pile temperature versus the elapsed time during the first thermal cycle of Test T40TM_30.

For the sake of brevity, only the results of test T40TM_30 are discussed here in detail. Pile head displacement measurements of the eight other thermo-mechanical tests show a trend similar to that of test T40TM_30. In order to provide detailed insight into the transient response of model pile during heating, cooling and recovery phases, thermally-induced axial and horizontal displacements of pile head are plotted versus the elapsed time along with temperature changes during 10 thermal cycles of test T40TM_30 in Figs. 5 and 6, respectively. It is worth mentioning that the positive and negative values of the axial displacement measurements represent the downward (i.e. settlement) and upward movement (i.e. heave) of the pile head, respectively. In addition, in Figs. 5-8, the displacements are solely thermally-induced; i.e., displacement readings at the pile head are zeroed before the beginning of the thermal loading.

As can be seen from Fig. 5, during the first thermal cycle, the heating phase did not lead to axial displacement at the pile head, while the cooling phase causes a continuous pile head settlement of up to 0.13%D. With increasing the number of thermal cycles, the pile head tends to move slightly upward with increasing temperature to 23℃ in the heating phase. Meanwhile, during cooling the pile temperature to the ambient temperature (i.e. 22 ℃), the pile head does not move axially but with a further decrease in pile temperature to 21 ℃, the pile head begins to move downward with a settlement of approximately 0.06%D. Eventually, during the recovery phase of all thermal cycles,

there is no axial movement of the pile head. In the cooling phase of each thermal cycle, the settlement/temperature slope is similar to that of the free thermal expansion/contraction curve (i.e. equal to α_m), which corresponds to the thermally-induced axial displacement of a fully toe-restrained pile being free to move in other directions. This trend is consistent with those obtained from previous experimental studies on dry sand [26,27,29].

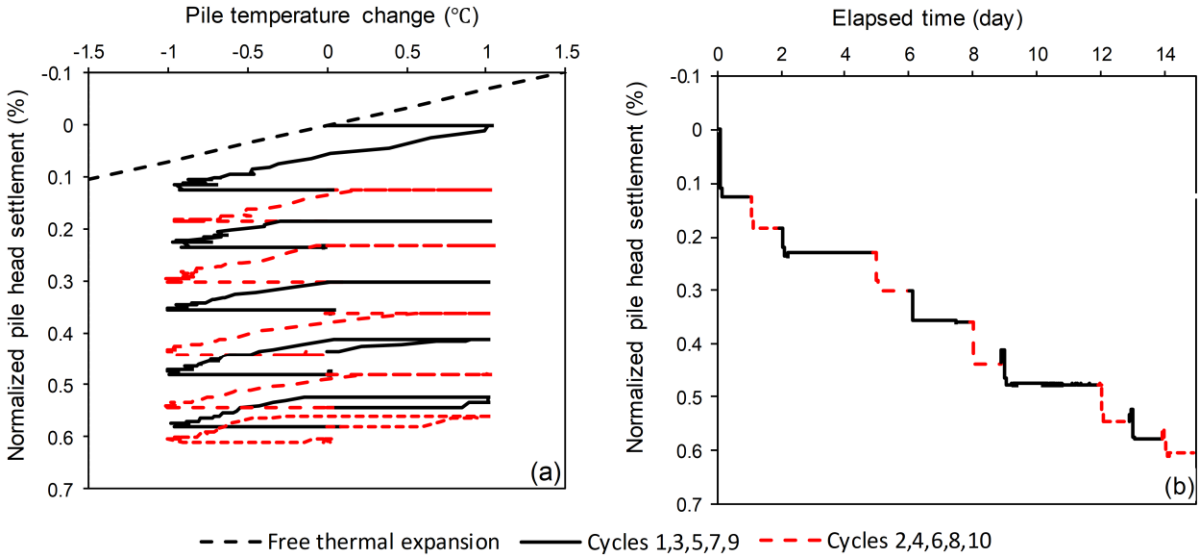

Fig. 5. Thermally-induced pile head settlement versus (a) temperature changes and (b) elapsed time during ten heating-cooling cycles of test T40TM_30.

In Fig. 6, generally, it can be observed that the pile head horizontal displacement increases continuously throughout each heating-cooling cycle. However, the rate of increase of the pile head horizontal displacement due to the cooling phase is negligible and could be ignored compared to that due to the heating phase. When the number of thermal cycles increases, the model pile tends to move less in the horizontal direction during the recovery phase, so that for the last few thermal cycles, the horizontal displacement could be neglected when compared to the one taking place during the heating phase. As can be seen from Fig. 6, for the first thermal cycle, the pile head initially moves horizontally by about 0.063%D during the heating phase, and then it continues to move horizontally for another 0.007%D during the subsequent cooling phase. Afterward, during the recovery phase, the pile head horizontal displacement continues to increase, reaching a peak value of 0.22%D. Correspondingly, for the tenth thermal cycle, pile head moves horizontally to 0.053%D during the heating phase while it moves marginally during the subsequent cooling phase. Afterward, during the recovery phase, the pile head exhibits no horizontal displacement and stabilizes at 0.06%. This kind of phenomenon is similarly observed in available centrifuge observations for horizontally-

loaded energy pile [19], where the pile head movement in the horizontal direction increases clearly during the heating cycle and it remains approximately unchanged during the subsequent cooling phase.

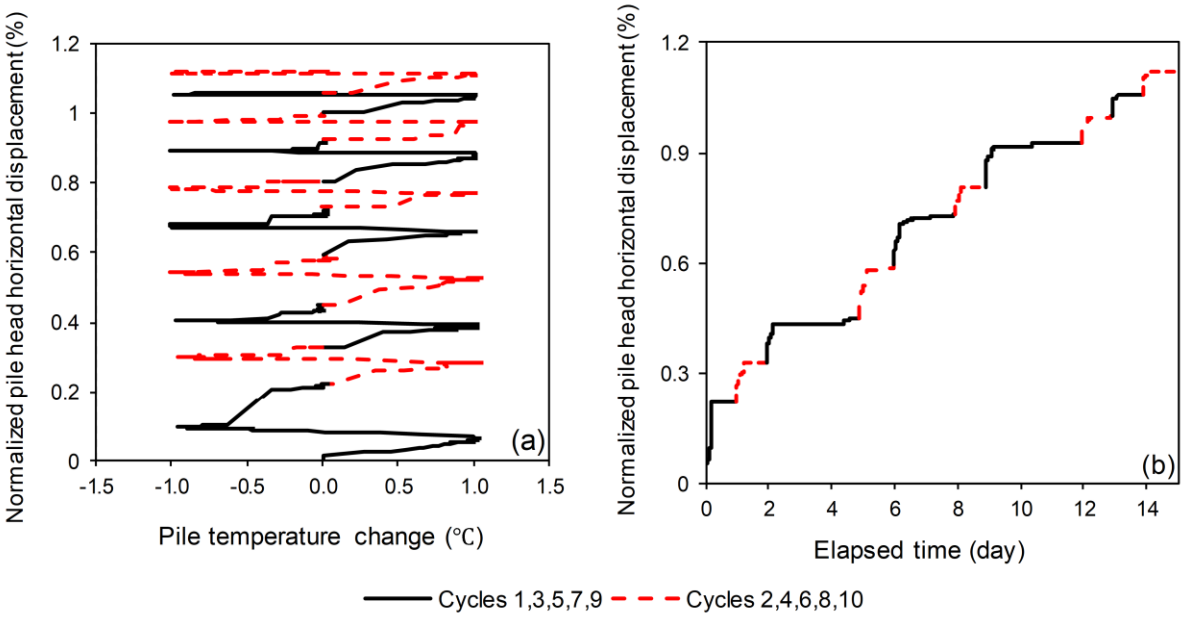

Fig. 6. Thermally-induced pile head horizontal displacement versus (a) temperature changes and (b) elapsed time during ten heating-cooling cycles of test T40TM_30.

It can be also noticed from Figs. 5 and 6 that although the pile has been subjected to some constant temperature for a long time in some thermal cycles due to continuing tests during weekends, its settlement and horizontal displacement are nearly stabilized. By the end of each thermal cycle, the model pile keeps settling and accumulating horizontal movement instead of returning to its initial position. This irreversible phenomenon may occur as a result of the cooling-induced radial contraction and constrained heating-induced downward expansion of the model pile accompanied by the thermally-induced volumetric contraction of surrounding sandy soil. When the surrounding soil experiences a volumetric contraction under the heating/cooling cycle (evidence of this phenomenon is available in previous works [36,39]) or when the model pile contracts radially under decreasing temperature, the lateral pressure acting on the pile shaft decreases, resulting in a reduction of the passive soil resistance as well as the shaft resistance. Since the surrounding soil is less resistant against the inclined mechanical loads, the amount of pile head horizontal displacement and pile toe settlement would increase to further mobilize the passive soil resistance in front of the pile and the base resistance at the pile toe.

The accumulated irreversible settlement and horizontal displacement of pile head are plotted against the number of thermal cycles in Fig. 7. In Fig. 7(a), the results show a general trend with a quick increase of normalized horizontal displacement during the first cycles and a continued increase at a smaller rate during the remaining cycles, which reaches 1.1-1.25%, 1.2-1.65% and 1.8-2.3% after ten cycles for the cases with F_h=*30%* Q_h, *50%* Q_h and *70%* Q_h, respectively. In Fig. 7(b), the results of Nguyen *et al* [29], using identical pile and soil, under axial load only (F_h = *0*) are also shown for comparison purposes. The results show that, for the cases with F_v = *10%* Q_v, irreversible normalized pile head settlement increases continuously and reaches 0.4% after ten cycles for F_h = *30%* Q_h (T10TM_30); for F_h = *50%* Q_h (T10TM_50) and F_h = *70%* Q_h (T10TM_70), it increases during the first three cycles and stabilizes at 0.13%. For the cases with F_v = *20%* Q_v, irreversible normalized pile head settlement increases continuously and reaches 0.43%, 0.23% and 0.2% after ten cycles for F_h = *0* (i.e. T20TM_0 [29]), F_h=*50%* Q_h (T20TM_50) and F_h = *70%* Q_h (T20TM_70), respectively, while for F_h = *30%* Q_h (T20TM_30), it rapidly increases during the first three cycles and tends to stabilize at 0.47%. Finally, for the cases with F_v = *40%* Q_v, irreversible normalized pile head settlement increases continuously and reaches 0.61%, 0.41% and 0.35% after ten cycles for F_h = *30%* Q_h (T40TM_30), F_h = *50%* Q_h (T40TM_50) and F_h = *70%* Q_h (T40TM_70), respectively. For the pure axial loading case with F_v = *40%* Q_v (i.e. T40TM_0 [29]), the accumulation rate of the irreversible settlement during the first two cycles is much higher than that in the cases of inclined loading; however, it decreases significantly during subsequent cycles and the accumulated irreversible normalized settlement stabilizes at 0.62% after ten cycles.

What should be noted from Fig. 7 is that for all the nine thermo-mechanical tests, regardless of the magnitude of the applied mechanical loads, the observed ratcheting pattern for axial and horizontal displacements is characterized by two features: first, the largest increment of irreversible settlement and horizontal displacement are induced by the first thermal cycle; second, after a fast accumulation of irreversible displacement in the first thermal cycle, the accumulation rate initially decreases slightly, and then almost remains constant when increasing the number of thermal cycles. The tendency for a model pile to exhibit less settlement and horizontal displacement with an increase in the number of thermal cycles is commonly explained by the strengthening of surrounding soil due to the thermally-induced gradual densification (which is a phenomenon observed in previous works [55]). This kind of ratcheting response was similarly observed for axially-loaded energy piles reported by Nguyen *et al* [29], Yavari *et al* [27] and Ng *et al* [39-41], and for horizontally-loaded energy pile reported by Zhao *et al* [19].

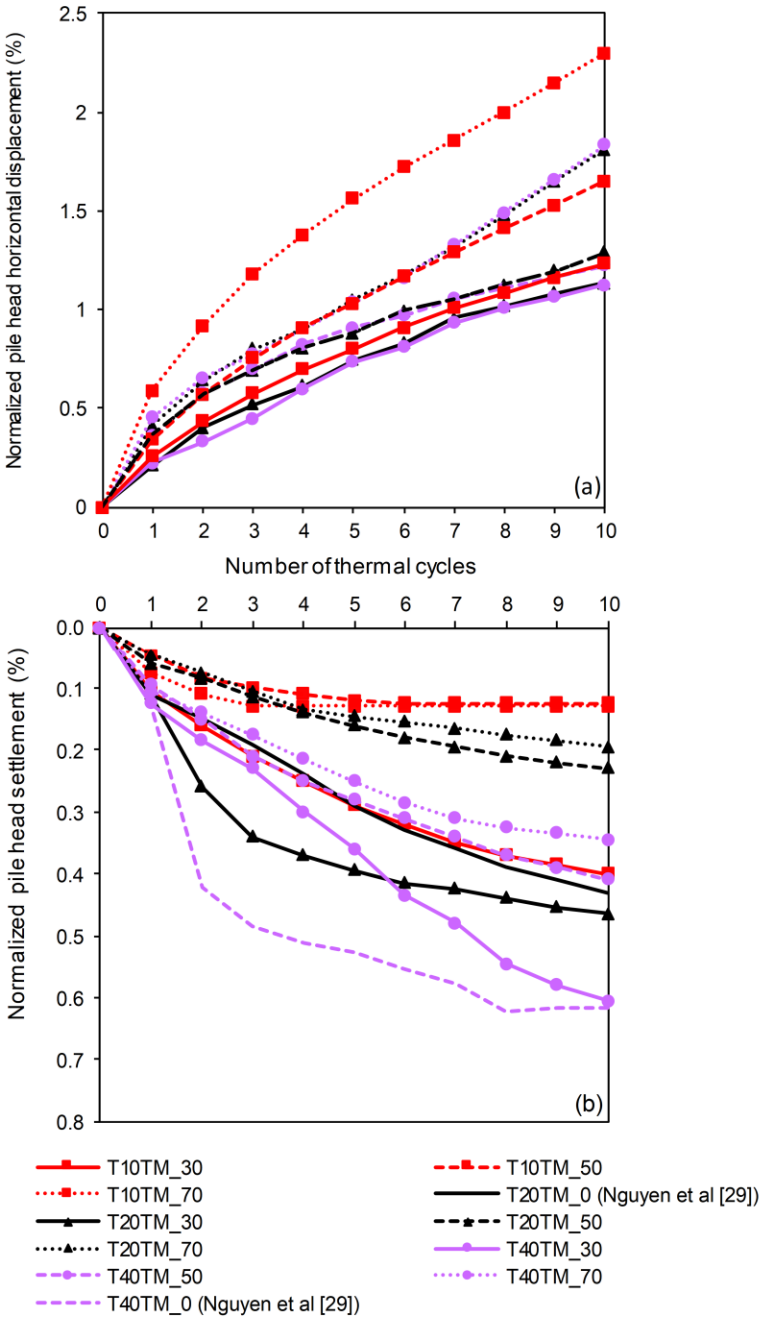

Fig. 7. (a) Irreversible horizontal displacements; (b) irreversible settlement of pile head versus the number of heating-cooling cycles.

3.3. Coupling effects on the thermally-induced mechanical response of model pile

Fig. 8 demonstrates the coupling effects on the irreversible settlement and horizontal displacements accumulated over ten heating/cooling cycles at the pile head.

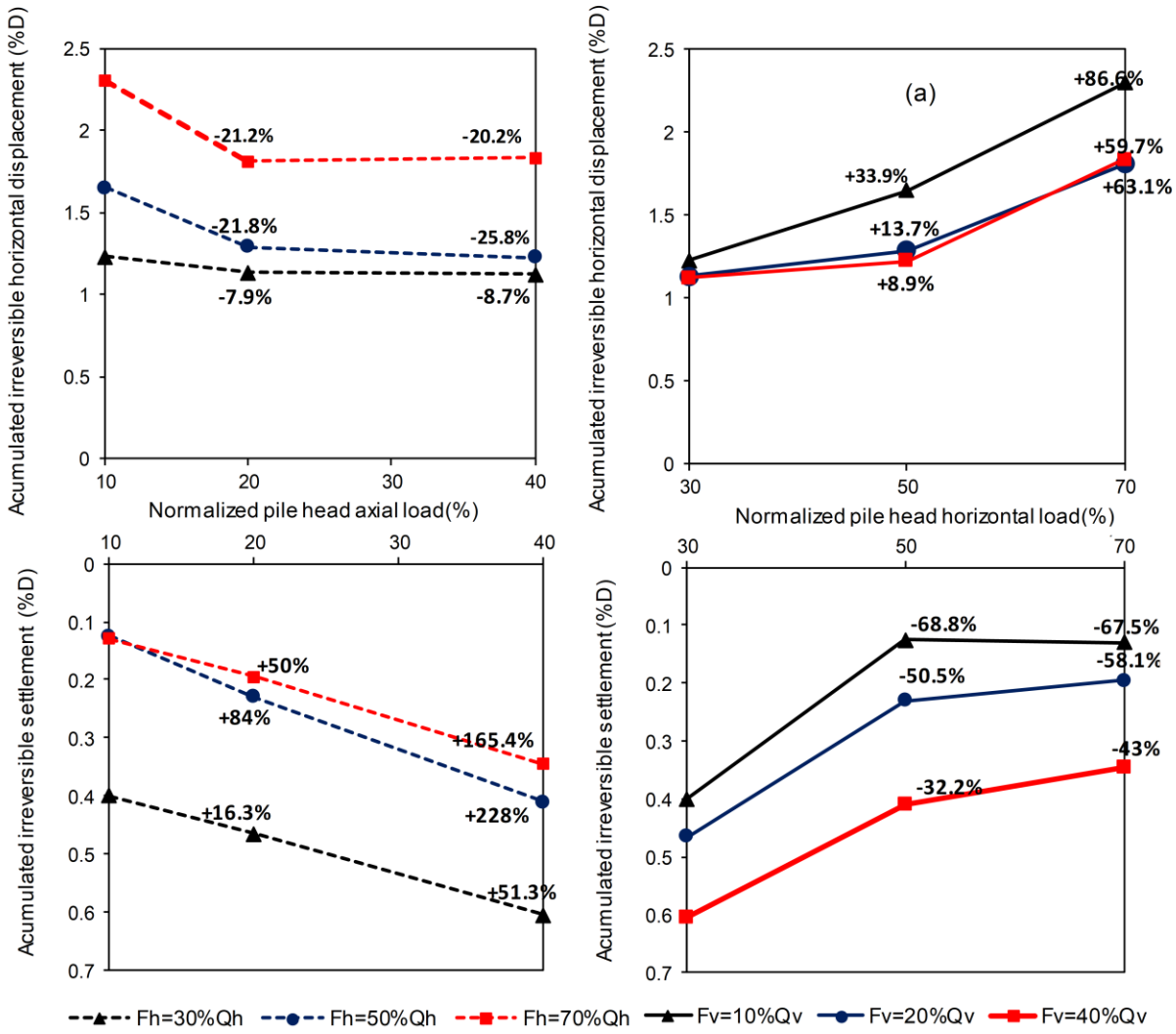

Fig. 8. Coupling effects on the irreversible settlement and horizontal displacement accumulated over ten heating/cooling cycles at the pile head.

As shown in Fig. 8, for the same horizontal load, imposing ten thermal cycles at an axial load higher than 10% Q_v induces a higher accumulated irreversible settlement of up to 228% but a lower accumulated irreversible horizontal displacement of up to 25.8%. For the same axial load, imposing ten thermal cycles at a horizontal load higher than 30% Q_h induces a lower accumulated irreversible settlement of up to 68.8% but a higher accumulated irreversible horizontal displacement of up to 86.6%. This possibly occurs because of the influence of mechanical loading condition on the soil-pile stiffness before the application of thermal loading. In general, it could be stated that at a specific axial load, the axial stiffness of the soil-pile system increases with an increase in horizontal load due to the increase in mobilized skin friction stresses, which result from increasing horizontal stresses and upward-directed

movement of passive earth pressure wedge in front of the pile. Moreover, at a specific horizontal load, the horizontal stiffness of the soil-pile system increases with the increasing axial load. This could be explained by the increase in mobilized passive earth pressure, which arises from increasing level of confinement provided by the surrounding soil due to the axial load-induced settlement of pile.

These results agree with those obtained for purely mechanical loading, in which the increase of axial load at the same horizontal load leads to a reduction in horizontal displacement, but an increase in the settlement; Moreover, the increase of horizontal load at the same axial load leads to an increase in horizontal displacement. Only the reduction of the accumulated irreversible settlement with the increase of horizontal load at the same axial load is contrary to that observed for purely mechanical loading. Since for the same axial load, the horizontal load increases in three steps, and ten thermal cycles are imposed to the pile at the end of each step (as described in section 2.2), the accumulated thermally-induced irreversible settlement under the horizontal loads of *50%* and *70%* Q_h might be influenced by the accumulated thermally-induced irreversible settlement induced by the horizontal loads of *30%* and *50%* Q_h.

3.4. Load-displacement response of model pile subjected to thermo-mechanical load

In order to investigate the influence of thermal loading on the pile response, the results obtained from the mechanical and thermo-mechanical experiments are presented in terms of normalized pile head horizontal displacement and settlement versus normalized horizontal load (i.e. divided by pile's ultimate horizontal load for the mechanical tests) in Fig. 9. As shown in Fig. 9, during the initial increase of F_h to 30% Q_h prior to the application of thermal loading, the settlement and horizontal displacement of pile head in thermo-mechanical tests are similar to those in mechanical ones. In the subsequent increments of the horizontal load to 50%, 70%, and 100% Q_h after the application of thermal loading, pile head horizontal displacement remains unchanged for a while and then increases again with increment rates equal to those in mechanical tests. Meanwhile, pile head settlement almost does not change with horizontal load increments after having been thermally loaded. When comparing the horizontal load-displacement response of the pile in mechanical experiments to those in thermo-mechanical ones, it must be pointed out that the thermal loading does not affect the horizontal response of the soil-pile system. The reason for this is that the large extent of reduction in the horizontal stress and mobilized skin friction is recovered by the subsequent

reloading phase. Therefore, it could be concluded that the total axial and lateral resistance of the pile is affected only slightly by the thermal loading. By comparing the horizontal load at a pile head horizontal displacement of 4 mm (i.e. 20% pile diameter), the ultimate horizontal bearing capacity of pile may remain unchanged after ten heating-cooling cycles. However, due to the gradual accumulation of the irreversible pile head horizontal displacement over thermal cycles, it is recommended that the long-term performance of the energy pile is controlled by horizontal displacement rather than ultimate horizontal bearing capacity.

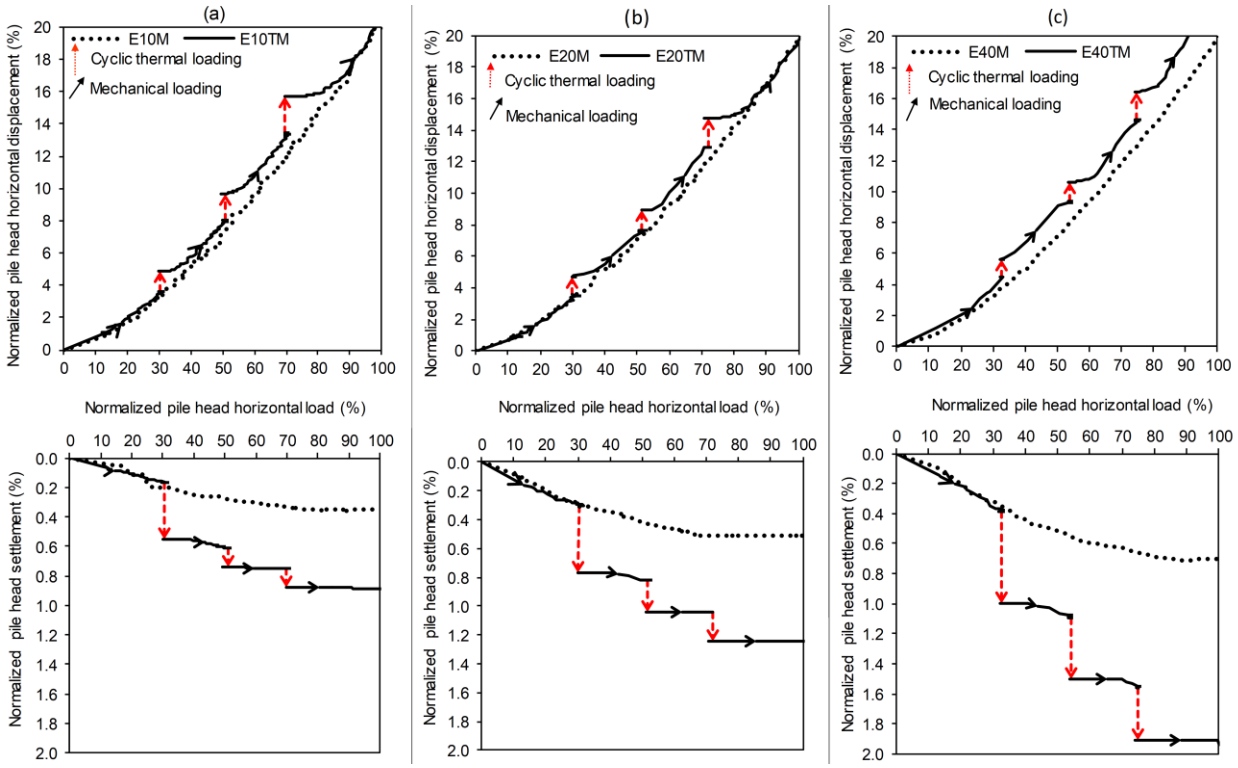

Fig. 9. Temperature-induced change in pile head response to horizontal load under a constant axial load of (a) 10% (b) 20% and (c) 40% of the axial pile resistance.

4. Conclusions

The thermo-mechanical behavior of a model energy pile subjected to inclined mechanical loads and temperature variations was experimentally investigated in dry sand. Ten heating-cooling cycles were applied to the pile under various combination of axial and horizontal mechanical loading (axial loads equal to 10, 20, and 40% of the ultimate axial load; horizontal loads equal to 30, 50, and 70% of the ultimate horizontal load). The main conclusions that can be drawn from this study are the following:

- For $Fv \leq 40\%Qv$, effect of Fv on the horizontal response of the pile under horizontal loading could be considered negligible. Moreover, additional settlement occurs at pile head due to the horizontal loading.
- The application of temperature variations along with inclined mechanical loads results in irreversible settlement and horizontal displacement at the pile head, whose largest increment takes place during the first thermal cycle. After a fast accumulation of irreversible displacement in the first thermal cycle, the increments of irreversible settlement and horizontal displacement, accumulating after each thermal cycle, initially decrease slightly and then almost remain constant with an increase in the number of heating-cooling cycles. By the end of the tenth thermal cycle, the amount of accumulated irreversible settlement and horizontal displacement are generally in the range of 0.1-0.6%D and 1.1-2.3%D, respectively.
- Under the same horizontal load, thermal cycles at a higher axial load induce a higher irreversible settlement but a lower horizontal displacement at the pile head.
- Under the same axial load, thermal cycles at a higher horizontal load induce a lower settlement but a higher horizontal displacement at the pile head.
- Thermal loading did not affect the subsequent horizontal load-displacement response of the pile. Likewise, by comparing the horizontal load at a pile head horizontal displacement of 4 mm (i.e. 20%D), the ultimate horizontal bearing capacity of the pile remained barely unchanged after ten heating-cooling cycles. However, due to the accumulation of irreversible horizontal displacement during the cyclic thermal loading, it is vital to ensure that the long-term cyclic thermal loading does not degrade the safety and durability of the energy piles for the service life of the building. Therefore, it is highly recommended that the long-term performance of the energy pile is controlled by horizontal displacement rather than ultimate horizontal bearing capacity.

The results of 1-g model tests carried out in this study could be helpful to gain insights into the qualitative influence of inclined mechanical loading on the thermally-induced displacements in both axial and horizontal directions; however, in order to provide quantitative confirmation of these initial findings, further studies are required to be conducted using centrifuge and field-scale tests.

Declarations

Data availability and materials

The data that support the findings of this study are available from the corresponding author on reasonable request.

Conflict of Interest

The authors declare that they have no known competing for financial interests or personal relationships that could have appeared to influence the work reported in this paper.

References

[1] Brandl H (2006) Energy foundations and other thermo-active ground structures. Géotechnique 56(2):81–122. https://doi.org/10.1680/geot.2006.56.2.81.

[2] Laloui L, Nuth M, Vulliet L (2006) Experimental and numerical investigations of the behaviour of a heat exchanger pile. Int. J. Numer. Anal. Methods Geomech.30:763–781. https://doi.org/10.1002/nag.499.

[3] Adam D, Markiewicz R (2009) Energy from earth-coupled structures, foundations, tunnels and sewers. Géotechnique 59(3):229–236. https://doi.org/10.1680/geot.2009.59.3.229.

[4] Loveridge FA, Powrie W (2013) Performance of piled foundations used as heat exchangers. *In: Proceedings of the 18th International Conference on Soil Mechanics and Geotechnical Engineering*, Paris, pp 2-5.

[5] Loveridge FA, Powrie W (2013) Temperature response functions (G-functions) for single pile heat exchangers. Energy 57:554– 564. https://doi.org/10.1016/j.energy.2013.04.060.

[6] Loveridge FA, Powrie W, Amis T, Wischy M, Kiauk J (2016) Long term monitoring of CFA energy pile schemes in the UK. *In: Proceedings of the 1st International Conference Energy Geotechnics*, Kiel, pp 585-592. https://doi.org/10.1201/b21938-92.

[7] Loveridge FA, McCartney JS, Narsilio GA, Sanchez M (2020) Energy geostructures: a review of analysis approaches, in situ testing and model scale experiments. Geomech. Energy Environ. 22:100173. https://doi.org/10.1016/j.gete.2019.100173.

[8] Jain NK, Ranjan G, Ramasamy G (1987) Effect of vertical load on flexural behavior of piles. Geotech. Eng. 18(2):185-204.

[9] Lee J, Prezzi M, Salgado R (2011) Experimental investigation of the combined load response of model piles driven in sand. *J. Geotech. Test.* 34(6):653–667. https://doi.org/10.1520/GTJ103269.

[10] Lee J, Prezzi M, Salgado R (2013) Influence of axial loads on the lateral capacity of instrumented steel model piles. *Int. J. Pave. Res. Tech.* 6(2):80-85. https://doi.org/10.6135/ijprt.org.tw/2013.6(2).80.

[11] Mu L, Kang X, Feng K, Huang M, Cao J (2018) Influence of vertical loads on lateral behaviour of monopoles in sand. *Eur. J. Environ. Civ. Eng.* 22(sup1): s286-s301. https://doi.org/10.1080/19648189.2017.1359112.

[12] Xu D, Huang F, Rui R (2020) Investigation of single pipe pile behavior under combined vertical and lateral loadings in standard and coral sands. *Int. J. Geosynth. Ground Eng.* 6:20. https://doi.org/10.1007/s40891-020-00203-4.

[13] Zhang XL, Xue JY, Han Y, Chen SL (2021) Model test study on horizontal bearing behavior of pile under existing vertical load. *Soil Dyn. and Earthq. Eng*. 147:106820. https://doi.org/10.1016/j.soildyn.2021.106820.

[14] Lu W, Zhang G (2018) Influence mechanism of vertical-horizontal combined loads on the response of a single pile in sand. *Soils Found*. 58(5):1228-1239. https://doi.org/10.1016/j.sandf.2018.07.002.

[15] Bartolomey AA (1977) Experimental Analysis of Pile Groups under Lateral Loads. *In: Proceedings of the 9th International Conference on Soil Mechanics and Foundation Engineering*, Tokyo, pp 187-188.

[16] Karasev OV, Talanov GP, Benda SF (1977) Investigation of the Work of Single Situ-Cast Piles under Different Load Combinations. *Soil Mech. Found. Eng*. 14(3):173-177.

[17] Zhukov NV, Balov IL (1978) Investigation of the Effect of a Vertical Surcharge on Horizontal Displacements and Resistance of Pile Columns to Horizontal Loads. *Soil Mech. Found. Eng*. 15(1):16-22.

[18] Vitali D, Leung AK, Feng S, Knappett JA, Ma L (2021) Centrifuge modelling of the use of discretely-spaced energy pile row to reinforce unsaturated silt. *Géotechnique* (In press). https://doi.org/10.1680/jgeot.20.P.157.

[19] Zhao R, Leung AK, Knappett JA (2022) Thermally induced ratcheting of a thermo-active reinforced concrete pile in sand under sustained lateral load. *Géotechnique* (In press). https://doi.org/10.1680/jgeot.21.00299

[20] Wang B, Bouazza A, Singh RM, Haberfield C, Barry-Macaulay D, Baycan S (2015) Posttemperature effects on shaft capacity of a full-scale geothermal energy pile. *J. Geotech. Geoenviron. Eng.* 141(4):04014125. https://doi.org/10.1061/(ASCE)GT.1943-5606.0001266.

[21] McCartney JS, Murphy KD (2017) Investigation of potential dragdown/uplift effects on energy piles. *Geomech. Energy Environ.* 10:21-28. https://doi.org/10.1016/j.gete.2017.03.001.

[22] Faizal M, Bouazza A, Haberfield C, McCartney JS (2018) Axial and radial thermal responses of a field-scale energy pile under monotonic and cyclic temperature changes. *J. Geotech. Geoenviron. Eng.* 144(10):04018072. https://doi.org/10.1061/(ASCE)GT.1943-5606.0001952.

[23] Faizal M, Bouazza A, McCartney JS, Haberfield C (2019) Effects of cyclic temperature variations on thermal response of an energy pile under a residential building. *J. Geotech. Geoenviron. Eng*. 145(10):04019066. https://doi.org/10.1061/(ASCE)GT.1943-5606.0002147.

[24] Sutman M, Brettmann T, Olgun G (2019) Full-scale in-situ tests on energy piles: Head and base-restraining effects on the structural behaviour of three energy piles. *Geomech. Energy Environ.* 18:56-68. https://doi.org/10.1016/j.gete.2018.08.002.

[25] Jiang G, Lin C, Shao D, Huang M, Lu H, Chen G, Zong C (2021) Thermo-mechanical behavior of driven energy piles from full-scale load tests. *Energy Build.* 233:110668**.** https://doi.org/10.1016/j.enbuild.2020.110668.

[26] Kalantidou A, Tang AM, Pereira JM, Hassen G (2012) Preliminary study on the mechanical behaviour of heat exchanger pile in physical model. *Géotechnique* 62(11):1047–1051. https://doi.org/10.1680/geot.11.T.013.

[27] Yavari N, Tang AM, Pereira JM, Hassen G (2014) Experimental study on the mechanical behaviour of a heat exchanger pile using physical modelling. *Acta Geotech.* 9:385–398. https://doi.org/10.1007/s11440-014-0310-7.

[28] Yavari N, Tang AM, Pereira JM, Hassen G (2016) Mechanical behaviour of a small-scale energy pile in saturated clay. *Géotechnique* 66(11):878–887. https://doi.org/10.1680/geot/15-7-026.

[29] Nguyen VT, Tang AM, Pereira JM (2017) Long-term thermomechanical behavior of energy pile in dry sand. *Acta Geotech.*12:729–737. https://doi.org/10.1007/s11440-017-0539-z.

[30] Nguyen VT, Wu N, Gan Y, Pereira JM, Tang AM (2020) Long-term thermo-mechanical behaviour of energy piles in clay. *Environ. Geotech*. 7(4):237-248. https://doi.org/10.1680/jenge.17.00106.

[31] Wang CL, Liu HL, Kong GQ, Ng CWW (2017) Different types of energy piles with heating-cooling cycles. *Proc. Inst. Civ. Eng. Geotech. Eng.* 170(3):220-231. https://doi.org/10.1680/jgeen.16.00061.

[32] Wu D, Liu HL, Kong GQ, Li C (2019) Thermo-mechanical behavior of energy pile under different climatic conditions. *Acta Geotech*. 14:1495-1508. https://doi.org/10.1007/s11440-018-0731-9.

[33] Fei K, Dai D (2018) Experimental and numerical study on the behavior of energy piles subjected to thermal cycles. *Adv. Civ. Eng.* 3424528. https://doi.org/10.1155/2018/3424528.

[34] Liu HL, Wang CL, Kong GQ, Bouazza A (2019) Ultimate bearing capacity of energy piles in dry and saturated sand. *Acta Geotech*. 14:869-879. https://doi.org/10.1007/s11440-018-0661-6.

[35] Bao X, Li Y, Feng T, Cui H, Chen X (2020) Investigation on thermo-mechanical behavior of reinforced concrete energy pile with large cross-section in saturated sandy soil by model experiments. *Undergr.* Space 5(3):229-241. https://doi.org/10.1016/j.undsp.2019.03.009.

[36] Kong GQ, Fang J, Huang X, Liu HL, Abuel-Naga H (2021) Thermal induced horizontal earth pressure changes of pipe energy piles under multiple heating cycles. *Geomech. Energy Environ.* 26:100228. https://doi.org/10.1016/j.gete.2020.100228.

[37] Stewart MA, McCartney JS (2014) Centrifuge modeling of soil-structure interaction in energy foundations. *J. Geotech. Geoenviron. Eng*. 140(4):04013044. https://doi.org/10.1061/(asce)gt.1943-5606.0001061.

[38] Ng CWW, Shi C, Gunawan A, Laloui L (2014) Centrifuge modelling of energy piles subjected to heating and cooling cycles in clay. *Géotech. Lett***.** 4(4):310–316. https://doi.org/10.1680/geolett.14.00063.

[39] Ng CWW, Shi C, Gunawan A, Laloui L, Liu HL (2015) Centrifuge modelling of heating effects on energy pile performance in saturated sand. *Can. Geotech. J.* 52(8):1045–1057. https://doi.org/10.1139/cgj-2014-0301.

[40] Ng CWW, Gunawan A, Shi C, MA QJ, Liu HL (2016) Centrifuge modelling of displacement and replacement energy piles constructed in saturated sand: a comparative study. *Géotech. Lett.* 6(1):34-38. https://doi.org/10.1680/jgele.15.00119.

[41] Ng CWW, Zhang C, Farivar A, Gomaa SMMH (2020) Scaling effects on the centrifuge modelling of energy piles in saturated sand. *Géotech. Lett*. 10(1):57-62. https://doi.org/10.1680/jgele.19.00051.

[42] Wood DM (2004) *Geotechnical modelling.* Spon Press, London.

[43] Das BM (2017) *Principle of Foundation Engineering.* Thomson/Brooks/Cole, Pacific Grove.

[44] Kraft L (1991) Performance of axially loaded pipe piles in sand. *J. Geotech. Geoenviron. Eng.*117(2):272-296.

[45] Boominathan A, Ayothiraman R (2006) An experimental study on static and dynamic bending behaviour of piles in soft clay. *Geotech. Geol. Eng*. 25:177. https://doi.org/10.1007/s10706-006-9102-7.

[46] LeBlanc C, Houlsby GT, Byrne BW (2010) Response of stiff piles in sand to long-term cyclic lateral loading. *Geotechnique* 60(2):79–90. https://doi.org/10.1680/geot.7.00196.

[47] Reddy KM, Ayothiraman R (2015) Experimental Studies on Behavior of Single Pile under Combined Uplift and Lateral Loading. *J. Geotech. Geoenviron. Eng.* 141(7):04015030. https://doi.org/10.1061/(ASCE)GT.1943-5606.0001314.

[48] Kramer CA, Ghasemi-Fare O, Basu P (2015) Laboratory Thermal Performance Tests on a Model Heat Exchanger Pile in Sand. *Geotech. Geol. Eng*. 33:253-271. https://doi.org/10.1007/s10706-014-9786-z.

[49] Arshad M, O'Kelly BC (2017) Model Studies on Monopile Behavior under Long-Term Repeated Lateral Loading. *Int. J. Geomech*. 17(1):04016040. https://doi.org/10.1061/(ASCE)GM.1943-5622.0000679.

[50] Feia S, Sulem J, Canou J, Ghabezloo S, Clain X (2016) Changes in permeability of sand during triaxial loading: effect of fine particles production. *Acta Geotech* 11:1-19. https://doi.org/10.1007/s11440-014-0351-y.

[51] Fioravante V (2002) On the shaft friction modelling of non-displacement piles in sand. *Soils Found.* 42(2):23–33.

[52] El Sawwaf M (2006) Lateral resistance of single pile located near geosynthetic reinforced slope. *Geotech. Geoenviron. Eng.* 132(10):1336–1345. https://doi.org/10.1061/(ASCE)1090-0241(2006)132:10(1336).

[53] You S, Cheng X, Guo H, Yao Z (2016) Experimental study on structural response of CFG energy piles. *Appl. Therm. Eng*. 96(5):640-651. https://doi.org/10.1016/j.applthermaleng.2015.11.127.

[54] Zhao R, Leung AK, Vitali D, Knappett JA (2020) Small-scale modeling of thermomechanical behavior of reinforced concrete energy piles in soil. *J. Geotech. Geoenviron. Eng.* 146(4):04020011. https://doi.org/10.1061/(ASCE)GT.1943-5606.0002225.

[55] Blanc B, Géminard JC (2013) Intrinsic creep of a granular column subjected to temperature changes. Phys. Rev. E 88(2):022201. https://doi.org/10.1103/PhysRevE.88.022201.